Supplementary Information: Unconventional Resistivity Scaling in Topological Semimetal CoSi

Shang-Wei Lien†,[1] Ion Garate†*,[2] Utkarsh Bajpai,[3] Cheng-Yi Huang,[4] Chuang-Han Hsu,[5] Yi-Hsin Tu,[1] Nicholas A. Lanzillo,[3] Arun Bansil,[4] Tay-Rong Chang,[1,6,7] Gengchiau Liang*,[8] Hsin Lin*,[5] and Ching-Tzu Chen*[9]

[1] *Department of Physics, National Cheng Kung University, Tainan 701, Taiwan.*

[2] *Département de physique, Institut quantique and Regroupement Québécois sur les Matériaux de Pointe, Université de Sherbrooke, Sherbrooke, Québec, Canada J1K 2R1.*

[3] *IBM Research, 257 Fuller Road, Albany, NY 12203, USA.*

[4] *Department of Physics, Northeastern University, Boston, Massachusetts 02115, USA.*

[5] *Institute of Physics, Academia Sinica, Nankang Taipei 11529, Taiwan, Republic of China.*

[6] *Center for Quantum Frontiers of Research and Technology (QFort), Tainan 701, Taiwan.*

[7] *Physics Division, National Center for Theoretical Sciences, Hsinchu, Taiwan.*

[8] *Department of Electrical and Computer Engineering, Faculty of Engineering, National University of Singapore, Singapore, Singapore.*

[9] *IBM T.J. Watson Research Center, 1101 Kitchawan Road, Yorktown Heights, NY 10598, USA.*

(Dated: December 15, 2022)

†these authors contributed equally

*corresponding authors.

Email: ion.garate@usherbrooke.ca; elelg@nus.edu.sg; nilnish@gate.sinica.edu.tw; cchen3@us.ibm.com

Supplementary Discussion: Analytical theory of the resistivity scaling and relaxation lengths in CoSi films

In this section, we begin by adapting the theory of Breitkreiz and Brouwer [PRL **123**, 066804 (2019)] to calculate the bulk and surface contributions to the three dimensional current density in CoSi films. The validity of this theory is limited to thicker films, where the surface and the bulk states are well differentiated.

Then, we go beyond the theory of Breitkreiz and Brouwer by providing microscopic (Fermi golden rule) expressions for the relaxation lengths. In the main text, these expressions are computed using first-principles electronic structure methods. In addition, these expressions allow to compare the analytical theory of the resistivity scaling with the fully numerical results based on Kubo's formula.

Generalities

We consider a film with spatial dimensions $L_x \times d \times L_z$ (see Supplementary Figure 1), where L_x and L_z are assumed to be much larger than the film thickness d.

In the bulk, CoSi hosts Fermi pockets around the Γ, R and M points of the three dimensional Brillouin zone. Unlike in the model considered by Breitkreiz and Brouwer, CoSi cannot be separated into two coupled subsystems that are related to one another by time-reversal. We will instead consider that the bulk is composed of three subsystems, with

Supplementary Figure 1: CoSi film connected to source and drain electrode

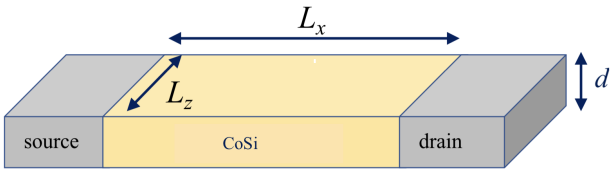

low-energy fermions near Γ, R and M. Each subsystem is invariant under time-reversal (because Γ, R and M are time-reversal-invariant momenta).

At the surface, CoSi hosts Fermi arcs. There are two Fermi arcs on the $y = d/2$ surface, denoted as s and $\bar{s}$, which connect the projections of the Γ and R points on the surface Brillouin zone. The group velocities of the two arcs are opposite to one another, due to time-reversal symmetry. For simplicity, we will assume these velocities to be constant (independent of momentum). Then, there are two more arcs at the $y = -d/2$ surface. These arcs have the opposite group velocities to the ones on the $y = d/2$ surface.

Continuity equations

The current densities in the bulk (in $\mathrm{A/m^2}$) can be written as

$$\begin{aligned} \mathbf{j}_\Gamma &= eD_\Gamma n_\Gamma \boldsymbol{\nabla}\mu_\Gamma \\ \mathbf{j}_R &= eD_R n_R \boldsymbol{\nabla}\mu_R \\ \mathbf{j}_M &= eD_M n_M \boldsymbol{\nabla}\mu_M, \end{aligned} \tag{1}$$

where D_α, n_α and μ_α are the diffusion constants, the Fermi level density of states and the deviations of the electrochemical potentials from the equilibrium Fermi energy, respectively, at sector $\alpha = \Gamma, R, M$. We assume a diffusive transport in the bulk.

The surface current densities (in A/m) are

$$\begin{aligned} j_{s,\pm} &= \pm e n_s v \mu_{s,\pm} \\ j_{\bar{s},\pm} &= \mp e n_s v \mu_{\bar{s},\pm}, \end{aligned} \tag{2}$$

where $\pm$ stands for $y = \pm d/2$ surfaces, n_s is the density of states of Fermi arcs at the Fermi energy, v is the absolute value of the (constant) group velocity of surface electrons, and $\mu_{s\pm}$ is the deviation of the surface electrochemical potential from the equilibrium Fermi energy in the $y = \pm d/2$ surface. The surface states $s+$ and $\bar{s}+$ (or $s-$ and $\bar{s}-$) are related by time-reversal symmetry.

We assume that we apply a uniform electric field E_x in the x direction. We want to find out the expressions for the bulk and surface current in terms of E_x. This requires finding how all the $\mu-$s depend on E_x. To do so, we need

to solve the following set of continuity equations (which are adapted from the theory of Breitkreiz and Brouwer):

$$\begin{aligned}
\boldsymbol{\nabla}\cdot\mathbf{j}_\Gamma &= en_s v\left[\frac{\mu_\Gamma-\mu_{s,+}}{l_{s\Gamma}}+\frac{\mu_\Gamma-\mu_{\bar{s},+}}{l_{s\Gamma}}\right]\delta(y-d/2)\\
&\quad+en_s v\left[\frac{\mu_\Gamma-\mu_{s,-}}{l_{s\Gamma}}+\frac{\mu_\Gamma-\mu_{\bar{s},-}}{l_{s\Gamma}}\right]\delta(y+d/2)+en_\Gamma v\left[\frac{\mu_\Gamma-\mu_R}{l_{\Gamma R}}+\frac{\mu_\Gamma-\mu_M}{l_{\Gamma M}}\right] \qquad (3a)\\
\boldsymbol{\nabla}\cdot\mathbf{j}_R &= en_s v\left[\frac{\mu_R-\mu_{s,+}}{l_{sR}}+\frac{\mu_R-\mu_{\bar{s},+}}{l_{sR}}\right]\delta(y-d/2)\\
&\quad+en_s v\left[\frac{\mu_R-\mu_{s,-}}{l_{sR}}+\frac{\mu_R-\mu_{\bar{s},-}}{l_{sR}}\right]\delta(y+d/2)+en_\Gamma v\left[\frac{\mu_R-\mu_\Gamma}{l_{\Gamma R}}+\frac{\mu_R-\mu_M}{l_{RM}}\right] \qquad (3b)\\
\boldsymbol{\nabla}\cdot\mathbf{j}_M &= en_s v\left[\frac{\mu_M-\mu_{s,+}}{l_{sM}}+\frac{\mu_M-\mu_{\bar{s},+}}{l_{sM}}\right]\delta(y-d/2)\\
&\quad+en_s v\left[\frac{\mu_M-\mu_{s,-}}{l_{sM}}+\frac{\mu_M-\mu_{\bar{s},-}}{l_{sM}}\right]\delta(y+d/2)+en_\Gamma v\left[\frac{\mu_M-\mu_\Gamma}{l_{\Gamma M}}+\frac{\mu_M-\mu_R}{l_{RM}}\right] \qquad (3c)\\
\partial_x j_{s,\pm} &= en_s v\left[\frac{\mu_{s,\pm}-\mu_\Gamma(\pm d/2)}{l_{s\Gamma}}+\frac{\mu_{s,\pm}-\mu_R(\pm d/2)}{l_{sR}}+\frac{\mu_{s,\pm}-\mu_M(\pm d/2)}{l_{sM}}\right]\\
&\quad+en_s v\frac{\mu_{s,\pm}-\mu_{\bar{s},\pm}}{l_{s\bar{s}}}+en_s v\frac{\mu_{s,\pm}-\mu_{s,\mp}}{l_{\mathrm{tb}}}+en_s v\frac{\mu_{s,\pm}-\mu_{\bar{s},\mp}}{l_{\mathrm{tb}}} \qquad (3d)\\
\partial_x j_{\bar{s},\pm} &= en_s v\left[\frac{\mu_{\bar{s},\pm}-\mu_\Gamma(\pm d/2)}{l_{s\Gamma}}+\frac{\mu_{\bar{s},\pm}-\mu_R(\pm d/2)}{l_{sR}}+\frac{\mu_{\bar{s},\pm}-\mu_M(\pm d/2)}{l_{sM}}\right]\\
&\quad+en_s v\frac{\mu_{\bar{s},\pm}-\mu_{s,\pm}}{l_{s\bar{s}}}+en_s v\frac{\mu_{\bar{s},\pm}-\mu_{\bar{s},\mp}}{l_{\mathrm{tb}}}+en_s v\frac{\mu_{\bar{s},\pm}-\mu_{s,\mp}}{l_{\mathrm{tb}}}. \qquad (3e)
\end{aligned}$$

Equations (3a), (3b) and (3c) are the continuity equations for bulk electrons at Γ, R and M, respectively, in the steady state. The terms in the right hand side describe processes that break the conservation of the number of particles in sector α. For example, for the charge near Γ, an electron can jump onto one of the two surfaces (this is possible only in the immediate vicinity of the surfaces, as otherwise the matrix element for the transition vanishes), or it can jump either to R or to M Fermi pockets. The net rate of these jumps is proportional to the difference in electrochemical potentials between the different subsystems; this fact will be justified below from microscopic theory via the Fermi golden rule. The constant of proportionality contains the phenomenological relaxation lengths. We note that $\boldsymbol{\nabla}\cdot\mathbf{j}_\Gamma+\boldsymbol{\nabla}\cdot\mathbf{j}_R+\boldsymbol{\nabla}\cdot\mathbf{j}_M=0$ for all $y\neq\pm d/2$. This simply states that the total bulk charge must be conserved in the absence of surfaces.

Equations (3d) and (3e) describe the continuity equations for the surface electrons, in the steady state. Once again, the surface charge is not conserved due to the couplings between the Fermi arcs and the bulk sectors α. We have also incorporated direct coupling between the top and the bottom surface through the relaxation length l_{tb}. Time-reversal symmetry requires that $l_{\bar{s}\alpha}=l_{s\alpha}$ (recall that Γ, R and M are invariant under time-reversal, whereas s goes to $\bar{s}$ under time-reversal). The notation $\mu_\alpha(\pm d/2)$ stands for μ_α evaluated at $y=\pm d/2$.

Solution of continuity equations

We seek a solution of the form

$$\mu_\Gamma = eE_x x + \tilde{\mu}_\Gamma(y) \tag{4a}$$
$$\mu_R = eE_x x + \tilde{\mu}_R(y) \tag{4b}$$
$$\mu_M = eE_x x + \tilde{\mu}_M(y) \tag{4c}$$
$$\mu_{s,\pm} = eE_x x + \tilde{\mu}_{s,\pm}(y) \tag{4d}$$
$$\mu_{\bar{s},\pm} = eE_x x + \tilde{\mu}_{\bar{s},\pm}(y), \tag{4e}$$

where the $\tilde{\mu}$ are unknown functions of only y. The fact that μ_Γ, μ_R and μ_M contain $eE_x x$ makes sense because the bulk transport is assumed to be diffusive. The fact that $\mu_{s,\pm}$ and $\mu_{\bar{s},\pm}$ contains the same factor also makes sense since Fermi arcs are coupled to bulk states (it is assumed that the bulk-surface relaxation lengths are shorter than the channel length L_x).

We begin by determining the bulk electrochemical potentials. Combining Eqs. (1) and (4), we have

$$j_{\Gamma,x} = e^2 D_\Gamma n_\Gamma E_x \tag{5a}$$
$$j_{R,x} = e^2 D_R n_R E_x \tag{5b}$$
$$j_{M,x} = e^2 D_M n_M E_x \tag{5c}$$
$$j_{\Gamma,y} = eD_\Gamma n_\Gamma \partial_y \tilde{\mu}_\Gamma \tag{5d}$$
$$j_{R,y} = eD_R n_R \partial_y \tilde{\mu}_R \tag{5e}$$
$$j_{M,y} = eD_M n_M \partial_y \tilde{\mu}_M. \tag{5f}$$

For all $y \neq \pm d/2$, Eqs. (3a), (3b) and (3c) give

$$\begin{aligned}
\partial_y j_{\Gamma,y} &= en_\Gamma v \left[\frac{\tilde{\mu}_\Gamma - \tilde{\mu}_R}{l_{\Gamma R}} + \frac{\tilde{\mu}_\Gamma - \tilde{\mu}_M}{l_{\Gamma M}} \right] \\
\partial_y j_{R,y} &= en_\Gamma v \left[\frac{\tilde{\mu}_R - \tilde{\mu}_\Gamma}{l_{\Gamma R}} + \frac{\tilde{\mu}_R - \tilde{\mu}_M}{l_{RM}} \right] \\
\partial_y j_{M,y} &= en_\Gamma v \left[\frac{\tilde{\mu}_M - \tilde{\mu}_\Gamma}{l_{\Gamma M}} + \frac{\tilde{\mu}_M - \tilde{\mu}_R}{l_{RM}} \right],
\end{aligned} \tag{6}$$

where we used $\partial_x j_{\Gamma,x} = \partial_x j_{R,x} = \partial_x j_{M,x} = 0$ (because E_x is uniform). Combining Eqs. (5) and (6), we have

$$\begin{aligned}
\partial_y^2 \tilde{\mu}_\Gamma &= \frac{1}{\lambda_{\Gamma R}^2} (\tilde{\mu}_\Gamma - \tilde{\mu}_R) + \frac{1}{\lambda_{\Gamma M}^2} (\tilde{\mu}_\Gamma - \tilde{\mu}_M) \\
\partial_y^2 \tilde{\mu}_R &= \frac{1}{\lambda_{R\Gamma}^2} (\tilde{\mu}_R - \tilde{\mu}_\Gamma) + \frac{1}{\lambda_{RM}^2} (\tilde{\mu}_R - \tilde{\mu}_M) \\
\partial_y^2 \tilde{\mu}_M &= \frac{1}{\lambda_{M\Gamma}^2} (\tilde{\mu}_M - \tilde{\mu}_\Gamma) + \frac{1}{\lambda_{MR}^2} (\tilde{\mu}_M - \tilde{\mu}_R),
\end{aligned} \tag{7}$$

where we have defined

$$\begin{aligned}
\lambda_{\Gamma R} &= \sqrt{\frac{D_\Gamma l_{\Gamma R}}{v}} \\
\lambda_{\Gamma M} &= \sqrt{\frac{D_\Gamma l_{\Gamma M}}{v}} \\
\lambda_{R\Gamma} &= \sqrt{\frac{n_R D_R l_{\Gamma R}}{v n_\Gamma}} \\
\lambda_{RM} &= \sqrt{\frac{n_R D_R l_{RM}}{v n_\Gamma}} \\
\lambda_{M\Gamma} &= \sqrt{\frac{n_M D_M l_{\Gamma M}}{v n_\Gamma}} \\
\lambda_{MR} &= \sqrt{\frac{n_M D_M l_{RM}}{v n_\Gamma}}.
\end{aligned} \tag{8}$$

The general solution of Eq. (7) is cumbersome; we will not reproduce it here. Instead, we will impose constraints based on time-reversal symmetry, which greatly simplify the solution. In a time-reversal invariant system placed under a uniform electric field that points along a high-symmetry direction of the crystal, there cannot be any net transverse current density (at least to linear order in the electric field). Moreover, since Γ, R and M are time-reversal-invariant momenta, time-reversal symmetry implies $j_{\Gamma,y}(y) = -j_{\Gamma,y}(y)$, $j_{R,y}(y) = -j_{R,y}(y)$ and $j_{M,y}(y) = -j_{M,y}(y)$. Accordingly, $j_{\Gamma,y}(y) = j_{R,y}(y) = j_{M,y}(y) = 0$ for all y, and hence

$$\tilde{\mu}_\Gamma = \tilde{\mu}_R = \tilde{\mu}_M = \mu_0 = \text{const.} \tag{9}$$

The fact that the three bulk electrochemical potentials are identical to one another follows from the solution of Eq. (7) under the condition $\partial_y \mu_\alpha = 0$ for all α. It also makes sense from the fact that there is no chiral anomaly in the absence of an external magnetic field. Below, we will see that the value of μ_0 does not matter.

Next, we concentrate on the surface electrochemical potentials. Combining Eqs. (13), (3d), (3e), (4) and (9), we get

$$\begin{aligned}
\pm eE_x &= (\tilde{\mu}_{s,\pm} - \mu_0)\left(\frac{1}{l_{s\Gamma}} + \frac{1}{l_{sR}} + \frac{1}{l_{sM}}\right) + \frac{\tilde{\mu}_{s,\pm} - \tilde{\mu}_{\bar{s},\pm}}{l_{s\bar{s}}} + \frac{\mu_{s,\pm} - \mu_{s,\mp}}{l_{\text{tb}}} + \frac{\mu_{s,\pm} - \mu_{\bar{s},\mp}}{l_{\text{tb}}} \\
\mp eE_x &= (\tilde{\mu}_{\bar{s},\pm} - \mu_0)\left(\frac{1}{l_{s\Gamma}} + \frac{1}{l_{sR}} + \frac{1}{l_{sM}}\right) + \frac{\tilde{\mu}_{\bar{s},\pm} - \tilde{\mu}_{s,\pm}}{l_{s\bar{s}}} + e\frac{\mu_{\bar{s},\pm} - \mu_{\bar{s},\mp}}{l_{\text{tb}}} + \frac{\mu_{\bar{s},\pm} - \mu_{s,\mp}}{l_{\text{tb}}}.
\end{aligned} \tag{10}$$

Solving these equations, we get

$$\begin{aligned}
\tilde{\mu}_{s,\pm} &= \mu_0 \pm \frac{eE_x}{\frac{1}{l_{s\Gamma}} + \frac{1}{l_{sR}} + \frac{1}{l_{sM}} + \frac{2}{l_{s\bar{s}}} + \frac{2}{l_{\text{tb}}}} \\
\tilde{\mu}_{\bar{s},\pm} &= \mu_0 \mp \frac{eE_x}{\frac{1}{l_{s\Gamma}} + \frac{1}{l_{sR}} + \frac{1}{l_{sM}} + \frac{2}{l_{s\bar{s}}} + \frac{2}{l_{\text{tb}}}}.
\end{aligned} \tag{11}$$

Equations (4), (9) and (11) provide the complete solution for the electrochemical potentials. In order to check the

consistency of the solutions, let us integrate Eq. (3a) in the immediate vicinity of the $y = d/2$ surface, giving

$$j_{\Gamma,y}(d/2+0^+) - j_{\Gamma,y}(d/2-0^+) = en_s v\frac{\mu_\Gamma(d/2)-\mu_{s,+}}{l_{s\Gamma}} + en_s v\frac{\mu_\Gamma(d/2)-\mu_{\bar{s},+}}{l_{s\Gamma}}, \tag{12}$$

where 0^+ is an infinitesimal positive number. In view of our solutions for the chemical potentials, Eq. (12) simply yields $0 = 0$. The same conclusion applies if we integrate Eq. (3a) in the immediate vicinity of the $y = -d/2$ surface, or if we integrate either Eq. (3b) or Eq. (3c) in the immediate vicinity of either surface. In the calculation of Breitkreiz and Brouwer, this integration was necessary in order to fully determine the electrochemical potentials. In our present case, we have already determined them completely without having to do any boundary integral. Indeed, this boundary integral gives no new information in our case.

Surface vs bulk contributions to the average current density

We are now ready to write the final expressions for the currents. For example, the average contribution from Fermi arcs to the three dimensional current density is

$$j_s = \frac{j_{s,+}+j_{s,-}+j_{\bar{s},+}+j_{\bar{s},-}}{d} = \frac{4e^2 n_s v E_x}{d\left(\frac{1}{l_{s\Gamma}}+\frac{1}{l_{sR}}+\frac{1}{l_{sM}}+\frac{2}{l_{s\bar{s}}}+\frac{2}{l_{\mathrm{tb}}}\right)}. \tag{13}$$

For the range of film thicknesses that we consider, the direct surface-to-surface tunneling is weak and therefore $1/l_{\mathrm{tb}}$ can be neglected in Eq. (13). Moreover, using $n_s v = k_0/(2\pi h)$, where k_0 is the length of a straight line connecting the two ends of a Fermi arc in momentum space (see the Supplemental Material in the article of Breitkreiz and Brouwer), Eq. (13) can be rewritten as

$$j_s = \frac{2}{\pi h} e^2 k_0 \frac{l_s}{d} E_x, \tag{14}$$

where we have defined an effective surface relaxation length l_s via

$$\frac{1}{l_s} = \frac{1}{l_{s\Gamma}} + \frac{1}{l_{sR}} + \frac{1}{l_{sM}} + \frac{2}{l_{s\bar{s}}}. \tag{15}$$

In our case, $k_0 = \sqrt{2}\pi/a$, where a is the lattice constant of CoSi. We have quoted Eq. (14) in the discussion of Fig. 3 of the main text.

Thus, we find that in CoSi the contribution from Fermi arcs to the average three dimensional current density will be inversely proportional to the film thickness. This result matches qualitatively with that of Breitkreiz and Brouwer's result if we take $l_{b\bar{b}} \ll W$ in their theory ($l_{b\bar{b}}$ is the relaxation length between the time-reversed partner bulk states). This is perhaps not surprising, if one thinks of CoSi as two "glued" time-reversed partner subsystems.

The dimensionless ratio between the bulk and the (average) surface current densities reads

$$\frac{j_s}{j_b} = \frac{\sigma_s}{\sigma_b} = \frac{2}{\pi h} e^2 k_0 \frac{l_s}{d}\frac{1}{\sigma_b}, \tag{16}$$

where

$$\sigma_b = D_\Gamma n_\Gamma + D_R n_R + D_M n_M \tag{17}$$

is the conductivity of the bulk states.

The ratio σ_s/σ_b plays an important role in the interpretation of the Fig. 3 of the main text. For sufficiently small d, the surface current density is dominant and $\sigma_s > \sigma_b$. Conversely, as d gets larger, the relative importance of the bulk current density grows and $\sigma_s < \sigma_b$. To be more precise, in the theory of Fuchs and Sondheimer (see main text), the bulk conductivity scales as

$$\sigma_b \sim \sigma_0 \frac{1+p}{1-p} \frac{d}{l_0} \ln\left(\frac{l_0}{d}\right), \tag{18}$$

where l_0 is the 3D bulk mean free path, $p < 1$ is the probability of specular scattering at the surface, and σ_0 is the conductivity of an infinitely thick crystal ($\sigma_0 > \sigma_b$). This approximate expression holds for $l_0 \gg d$, which is the regime of interest in our case. We may estimate σ_0 by assuming that the main contribution to it comes from the Fermi pocket enclosing the R point (where the number of carriers is highest). Then, a simple estimate gives

$$\sigma_0 \sim \frac{e^2}{h} k_F^2 l_0, \tag{19}$$

where k_F is the Fermi wave vector of the bulk crystal for the Fermi pocket centered at R (which for the purposes of the estimate we take to be spherical). Accordingly,

$$\frac{\sigma_s}{\sigma_b} \sim \frac{1-p}{1+p} \frac{k_0 l_s}{(k_F d)^2 \ln\left(\frac{l_0}{d}\right)}. \tag{20}$$

Thus, the main factors enhancing the importance of the surface contribution to the average 3D conductivity are (i) long Fermi arcs ($k_0 \gg k_F$), (ii) long surface relaxation lengths ($l_s \gg d$) and (iii) thin films ($d \lesssim k_F^{-1}$). When the surface defect density N increases, p, l_0 and l_s all decrease, but it is the decrease of l_s that dominates the behavior of σ_s/σ_b as a function of N (see Supplementary Figures 4 and 6).

Fermi golden rule expressions for the relaxation lengths

Let us determine from microscopic theory the phenomenological relaxation lengths ($l_{s\bar{s}}$, $l_{s\Gamma}$, l_{sR} and l_{sM}) appearing in the preceding subsection. For concreteness, we will begin with the relaxation length $l_{s\Gamma}$ associated to the coupling between the bulk valley Γ and the surface band $s+$.

The *net* rate of charge transfer (in coulomb per second) from Γ to $s+$, due to static disorder, can be approximated by the Fermi's golden rule expression

$$\left(\frac{\partial Q}{\partial t}\right)_{\Gamma \to s+} - \left(\frac{\partial Q}{\partial t}\right)_{s+ \to \Gamma} = e\frac{2\pi}{\hbar} \sum_{n \in \Gamma} \sum_{n' \in s+} \sum_{\mathbf{k}} \sum_{\mathbf{k}'} |\langle n, \mathbf{k}|V|n', \mathbf{k}'\rangle|^2 \left(f_{n,\mathbf{k}} - f_{n',\mathbf{k}'}\right) \delta\left(\epsilon_{n,\mathbf{k}} - \epsilon_{n',\mathbf{k}'}\right), \tag{21}$$

where n and n' are the band labels for the Γ and $s+$ electrons (respectively), $|n, \mathbf{k}\rangle$ and $|n', \mathbf{k}'\rangle$ are the corresponding

eigenstates (note that $\mathbf{k}$ and $\mathbf{k}'$ are 2D momenta in the xz plane), V is the impurity potential, and $f_{n,\mathbf{k}} - f_{n',\mathbf{k}'}$ is the difference in electron occupation between states $(n,\mathbf{k})$ and $(n',\mathbf{k}')$. Assuming that the deviations from the equilibrium chemical potential are small, a Taylor expansion gives

$$\begin{aligned}\delta\left(\epsilon_{n,\mathbf{k}}-\epsilon_{n',\mathbf{k}'}\right)\left(f_{n,\mathbf{k}}-f_{n,\mathbf{k}'}\right) &\simeq \delta\left(\epsilon_{n,\mathbf{k}}-\epsilon_{n',\mathbf{k}'}\right)\left(\mu_{s+}-\mu_\Gamma\right)\frac{\partial}{\partial\epsilon_{n,\mathbf{k}}}\frac{1}{e^{\beta\left(\epsilon_{n,\mathbf{k}}-\epsilon_F\right)}+1}\\ &\simeq \left(\mu_\Gamma-\mu_{s+}\right)\delta\left(\epsilon_{n,\mathbf{k}}-\epsilon_{n',\mathbf{k}'}\right)\delta\left(\epsilon_{n,\mathbf{k}}-\epsilon_F\right)\\ &= \left(\mu_\Gamma-\mu_{s+}\right)\delta\left(\epsilon_{n',\mathbf{k}'}-\epsilon_F\right)\delta\left(\epsilon_{n,\mathbf{k}}-\epsilon_F\right),\end{aligned} \tag{22}$$

where ϵ_F is the Fermi energy in equilibrium and we have made a low-temperature approximation. Then, we have

$$\left(\frac{\partial Q}{\partial t}\right)_{\Gamma\to s+} - \left(\frac{\partial Q}{\partial t}\right)_{s+\to\Gamma} = \left(\mu_\Gamma-\mu_{s+}\right)e\frac{2\pi}{\hbar}\sum_{n\in\Gamma}\sum_{n'\in s+}\sum_{\mathbf{k}}\sum_{\mathbf{k}'}|\langle n,\mathbf{k}|V|n',\mathbf{k}'\rangle|^2\delta\left(\epsilon_{n,\mathbf{k}}-\epsilon_F\right)\delta\left(\epsilon_{n',\mathbf{k}'}-\epsilon_F\right). \tag{23}$$

On the other hand, the right hand side of the continuity equation Eq. (3a) leads to

$$\left(\frac{\partial Q}{\partial t}\right)_{\Gamma\to s+} - \left(\frac{\partial Q}{\partial t}\right)_{s+\to\Gamma} = \int d^3r\left[\left(\frac{\partial\rho}{\partial t}\right)_{\Gamma\to s+} - \left(\frac{\partial\rho}{\partial t}\right)_{s+\to\Gamma}\right] = \int d^3r\, en_s v\frac{\mu_\Gamma-\mu_{s,+}}{l_{s\Gamma}}\delta(y-d/2) = L_zL_x en_s v\frac{\mu_\Gamma-\mu_{s,+}}{l_{s\Gamma}}, \tag{24}$$

where ρ is the charge density ($\mathrm{C/m^3}$) and we have used the fact that $\mu_\Gamma-\mu_{s,+}$ is independent of x and z (note that both μ_Γ and $\mu_{s,+}$ depend on x, but their difference does not).

Identifying Eq. (23) with Eq. (24), we conclude that

$$\frac{en_s v}{l_{s\Gamma}} = \frac{1}{L_xL_z}e\frac{2\pi}{\hbar}\sum_{n\in\Gamma}\sum_{n'\in s+}\sum_{\mathbf{k}}\sum_{\mathbf{k}'}|\langle n,\mathbf{k}|V|n',\mathbf{k}'\rangle|^2\delta\left(\epsilon_{n,\mathbf{k}}-\epsilon_F\right)\delta\left(\epsilon_{n',\mathbf{k}'}-\epsilon_F\right). \tag{25}$$

The relaxation lengths l_{sR} and l_{sM} obey the same expression, upon replacing Γ by R and M (respectively). Similarly, we obtain

$$\frac{en_s v}{l_{s\bar{s}}} = \frac{1}{L_xL_z}e\frac{2\pi}{\hbar}\sum_{n\in s}\sum_{n'\in\bar{s}}\sum_{\mathbf{k}}\sum_{\mathbf{k}'}|\langle n,\mathbf{k}|V|n',\mathbf{k}'\rangle|^2\delta\left(\epsilon_{n,\mathbf{k}}-\epsilon_F\right)\delta\left(\epsilon_{n',\mathbf{k}'}-\epsilon_F\right). \tag{26}$$

For completeness, let us also discuss the bulk-to-bulk relaxation lengths (such as $l_{\Gamma R}$), even though they are not needed for our theory. The counterpart of Eq. (24) for these is

$$\left(\frac{\partial Q}{\partial t}\right)_{\Gamma\to R} - \left(\frac{\partial Q}{\partial t}\right)_{R\to\Gamma} = \int d^3r\left[\left(\frac{\partial\rho}{\partial t}\right)_{\Gamma\to R} - \left(\frac{\partial\rho}{\partial t}\right)_{R\to\Gamma}\right] = \int d^3r\, en_\Gamma v\frac{\mu_\Gamma-\mu_R}{l_{\Gamma R}} = L_xL_z den_\Gamma v\frac{\mu_\Gamma-\mu_\Gamma}{l_{\Gamma R}}, \tag{27}$$

which results in

$$\frac{en_\Gamma v}{l_{\Gamma R}} = \frac{1}{L_xL_z d}e\frac{2\pi}{\hbar}\sum_{n\in\Gamma}\sum_{n'\in R}\sum_{\mathbf{k}}\sum_{\mathbf{k}'}|\langle n,\mathbf{k}|V|n',\mathbf{k}'\rangle|^2\delta\left(\epsilon_{n,\mathbf{k}}-\epsilon_F\right)\delta\left(\epsilon_{n',\mathbf{k}'}-\epsilon_F\right). \tag{28}$$

Note that the dimensions are correct: n_s is the density of states per unit area of the surface states (an intensive quantity independent of system size unless the film is too thin) and n_Γ is the density of states per unit volume of the

bulk states (which is also an intensive quantity).

In the first principles calculations of the relaxation lengths (see main text) the impurity potential V is replaced by the T-matrix,

$$\frac{en_s v}{l_{s\Gamma}} = \frac{1}{L_x L_z} e \frac{2\pi}{\hbar} \sum_{n\in\Gamma} \sum_{n'\in s+} \sum_{\mathbf{k}} \sum_{\mathbf{k}'} |\langle n,\mathbf{k}|T|n',\mathbf{k}'\rangle|^2 \delta\left(\epsilon_{n,\mathbf{k}} - \epsilon_F\right) \delta\left(\epsilon_{n',\mathbf{k}'} - \epsilon_F\right)$$
$$\frac{en_s v}{l_{s\bar{s}}} = \frac{1}{L_x L_z} e \frac{2\pi}{\hbar} \sum_{n\in s} \sum_{n'\in \bar{s}} \sum_{\mathbf{k}} \sum_{\mathbf{k}'} |\langle n,\mathbf{k}|T|n',\mathbf{k}'\rangle|^2 \delta\left(\epsilon_{n,\mathbf{k}} - \epsilon_F\right) \delta\left(\epsilon_{n',\mathbf{k}'} - \epsilon_F\right). \tag{29}$$

together with $n_s v = k_0/(2\pi h)$ and $k_0 = \sqrt{2}\pi/a$. These expressions allow to go beyond the leading order in the impurity potential.

Fermi golden rule expression for the 3D bulk mean free path

Above, as well as in the main text, we make reference to the 3D bulk mean free path l_0. In this section, we provide a Fermi golden rule expression for l_0, which will allow us in the next subsection to determine how l_0 scales with the system size and impurity density.

The starting point is the elastic scattering rate for an electron in a bulk state $|n,\mathbf{k}\rangle$:

$$\frac{1}{\tau_{n,\mathbf{k}}} = \frac{2\pi}{\hbar} \sum_{\mathbf{k}',n'} |\langle n,\mathbf{k}|V|n',\mathbf{k}'\rangle|^2 \delta(E_{\mathbf{k},n} - E_{\mathbf{k}',n'}), \tag{30}$$

where $|n',\mathbf{k}\rangle$ are bulk states. Disregarding the distinction between transport and momentum scattering times (which is unimportant for our purposes below), the 3D bulk mean free path in a cubic crystal can be approximated with a Fermi-surface average of $v^x_{n,\mathbf{k}}\tau_{n,\mathbf{k}}$,

$$l_0 \simeq \frac{\sum_{\mathbf{k},n} v^x_{n,\mathbf{k}} \tau_{n,\mathbf{k}} \delta(\epsilon_F - E_{n,\mathbf{k}})}{\sum_{\mathbf{k},n} \delta(\epsilon_F - E_{n,\mathbf{k}})}, \tag{31}$$

where $v^x_{n,\mathbf{k}}$ is the $x-$component of the electronic group velocity in state $|n,\mathbf{k}\rangle$.

Scaling of relaxation lengths with impurity concentration and system size

To conclude this section, we analyze how the relaxation lengths from the preceding subsection vary with the film thickness. This scaling is useful to understand the numerical results shown in Figs. 3 and 4 of the main text. For concreteness, let us see how the surface-to-bulk relaxation length $l_{s\Gamma}$ scales with sample dimensions, when the latter are large. Later, we will adapt the arguments to other relaxation lengths of interest.

First, we write the Bloch states as

$$|n,\mathbf{k}\rangle = \frac{1}{\sqrt{L_x L_z d}} e^{i\mathbf{k}\cdot\mathbf{r}} |u_{n,\mathbf{k}}\rangle, \tag{32}$$

where $|u_{\mathbf{k},n}\rangle$ is the periodic part of the Bloch function (periodicity is present only in the xz plane), with normalization

$$1 = \langle n,\mathbf{k}|n,\mathbf{k}\rangle = \frac{1}{L_x L_z d}\int_{\text{all}} d^3r |u_{n,\mathbf{k}}(\mathbf{r})|^2 = \frac{N_{\text{cell}}}{L_x L_z d}\int_{\text{cell}} d^3r |u_{n,\mathbf{k}}(\mathbf{r})|^2 = \frac{1}{V_{\text{cell}}}\int_{\text{cell}} d^3r |u_{n,\mathbf{k}}(\mathbf{r})|^2, \tag{33}$$

where N_{cell} is the number of unit cells in the film and V_{cell} is the volume of a unit cell. From this equation, we conclude that $u_{n,\mathbf{k}}(\mathbf{r})$ does not scale with L_x, d and L_z for a bulk state, but $u_{n',\mathbf{k}'}(\mathbf{r}) \sim \sqrt{d}$ for the surface state. The reason for this is that, for a surface state, $u_{n',\mathbf{k}'}(\mathbf{r})$ has a finite range along y. Thus, $|u_{n',\mathbf{k}'}(\mathbf{r})|^2 \sim d$ is needed to cancel the $1/d$ factor coming from V_{cell} and to normalize the wave function to unity.

Second, we analyze the matrix element of the impurity potential. For a single short-range scatterer located at $\mathbf{r}_0$, $V(\mathbf{r}) = V_0\delta(\mathbf{r}-\mathbf{r_0})$ and

$$\langle n,\mathbf{k}|V|n',\mathbf{k}'\rangle = \frac{1}{L_x L_z d}\int_{\text{all}} e^{i(\mathbf{k}'-\mathbf{k})\cdot\mathbf{r}} V_0\delta(\mathbf{r}-\mathbf{r}_0) u^*_{n,\mathbf{k}}(\mathbf{r}) u_{n',\mathbf{k}'}(\mathbf{r}) = \frac{1}{L_x L_z d} V_0 e^{i(\mathbf{k}'-\mathbf{k})\cdot\mathbf{r}_0} u^*_{n,\mathbf{k}}(\mathbf{r}_0) u_{n',\mathbf{k}'}(\mathbf{r}_0). \tag{34}$$

Accordingly,

$$|\langle n,\mathbf{k}|V|n',\mathbf{k}'\rangle|^2 = \frac{V_0^2}{L_x^2 L_z^2 d^2}|u_{n,\mathbf{k}}(\mathbf{r}_0)|^2 |u_{n',\mathbf{k}'}(\mathbf{r}_0)|^2. \tag{35}$$

Importantly, this quantity is proportional to the probability of finding a bulk electron and a surface electron simultaneously at $\mathbf{r}_0$ (recall that n is a bulk state and n' is a surface state, since we are analyzing $l_{s\Gamma}$). With system size, it scales as

$$|\langle n,\mathbf{k}|V|n',\mathbf{k}'\rangle|^2 \sim \frac{1}{L_x^2 L_z^2 d}. \tag{36}$$

Third, consider N_{imp} short-range impurities, $V(\mathbf{r}) = V_0\sum_{i=1}^{N_{\text{imp}}}\delta(\mathbf{r}-\mathbf{r}_i)$. Assuming that these impurities are uncorrelated, the corresponding surface-to-bulk scattering rates can be added. Assuming that the impurities are randomly distributed in space with a density that is uniform on average, then only a fraction $N_{\text{imp}}r/d$ of them will contribute to $|\langle n,\mathbf{k}|V|n',\mathbf{k}'\rangle|^2$, where r is the range of the surface state wave function along the y direction. The remaining $N_{\text{imp}}(1-r/d)$ impurities will not overlap with the surface state wave function and thus will not contribute to $l_{s\Gamma}$. Thus, the matrix element for N_{imp} impurities scales as

$$|\langle n,\mathbf{k}|V|n',\mathbf{k}'\rangle|^2 \sim \frac{N_{\text{imp}}}{L_x^2 L_z^2 d^2}, \tag{37}$$

where we note that r is independent of sample dimensions when the latter are large.

Fourth, we recognize that (i) $\sum_{\mathbf{k}}$ and $\sum_{\mathbf{k}'}$ each scale as $L_x L_z$; (ii) $\sum_{n\in\Gamma}$ scales with d (because the number of quantum well states crossing the Fermi energy scales with the film thickness); (iii) $\sum_{n'\in s}$ does not scale with system size (since the number of Fermi arcs does not depend on the film thickness).

Combining the preceding four observations with Eq. (25), we conclude that

$$\frac{e n_s v}{l_{s\Gamma}} \sim \frac{1}{L_x L_z} L_x^2 L_z^2 d \frac{N_{\text{imp}}}{L_x^2 L_z^2 d^2} \sim \frac{N_{\text{imp}}}{L_x L_z d}. \tag{38}$$

Thus, $1/l_{s\Gamma}$ scales with the volume density of impurities. As mentioned above, these scaling arguments apply for

thicker films.

If we repeat the same scaling arguments for $l_{s\bar{s}}$, we find that

$$\frac{en_s v}{l_{s\bar{s}}} \sim \frac{N_{\text{imp}}}{L_x L_z d}, \tag{39}$$

i.e. $1/l_{s\bar{s}}$ is also proportional to the volume impurity density (assuming that those impurities are uniformly distributed in the entire film).

Finally, we can repeat similar arguments for the 3D bulk mean free path. Now the starting point is given by Eqs. (30) and (31). Using

$$|\langle n \in \text{bulk}, \mathbf{k}|V|n' \in \text{bulk}, \mathbf{k}'\rangle|^2 \sim \frac{N_{\text{imp}}}{L_x^2 L_z^2 d^2}, \tag{40}$$

the outcome reads

$$l_0^{-1} \sim \frac{N_{\text{imp}}}{L_x L_z d}, \tag{41}$$

i.e. the 3D bulk mean free path scales inversely with the volume density of impurities (which is of course well-known).

Thus far, we have assumed that the impurities were randomly but uniformly distributed across the entire film. In the main text, we consider the situation in which the vacancies are concentrated at the surfaces. All of those vacancies contribute to bulk-surface, surface-surface and bulk-bulk relaxation. This yields

$$\begin{aligned}
|\langle n \in s, \mathbf{k}|V|n' \in \Gamma, \mathbf{k}'\rangle|^2 &\sim \frac{N_{\text{imp}}^{\text{surf}}}{L_x^2 L_z^2 d} \to \frac{en_s v}{l_{s\Gamma}} \sim \frac{N_{\text{imp}}^{\text{surf}}}{L_x L_z} \equiv N \\
|\langle n \in s, \mathbf{k}|V|n' \in \bar{s}, \mathbf{k}'\rangle|^2 &\sim \frac{N_{\text{imp}}^{\text{surf}}}{L_x^2 L_z^2} \to \frac{en_s v}{l_{s\bar{s}}} \sim \frac{N_{\text{imp}}^{\text{surf}}}{L_x L_z} \equiv N \\
|\langle n \in \text{bulk}, \mathbf{k}|V|n' \in \text{bulk}, \mathbf{k}'\rangle|^2 &\sim \frac{N_{\text{imp}}^{\text{surf}}}{L_x^2 L_z^2 d^2} \to \frac{1}{l_0} \sim \frac{N_{\text{imp}}^{\text{surf}}}{L_x L_z d} \equiv \frac{N}{d},
\end{aligned} \tag{42}$$

where N is the areal density of surface vacancies. Thus, when impurities are localized on the surfaces, the surface-to-surface and bulk-to-surface scattering rates are independent of the film thickness and depend only on the areal density of impurities. However, the 3D bulk mean free path is inversely proportional to the film thickness[1]. Accordingly, if d is changed while N is kept fixed, then l_0 will also change. This change will nevertheless be often unimportant if there is in parallel another source of scattering (as modeled by the factor η in the main text), uniformly distributed in the bulk with a volume density that exceeds N/d.

---

[1] It is straightforward to show that this same statement applies to the bulk-to-bulk scattering lengths such as $l_{\Gamma R}$

Supplementary Figure 2

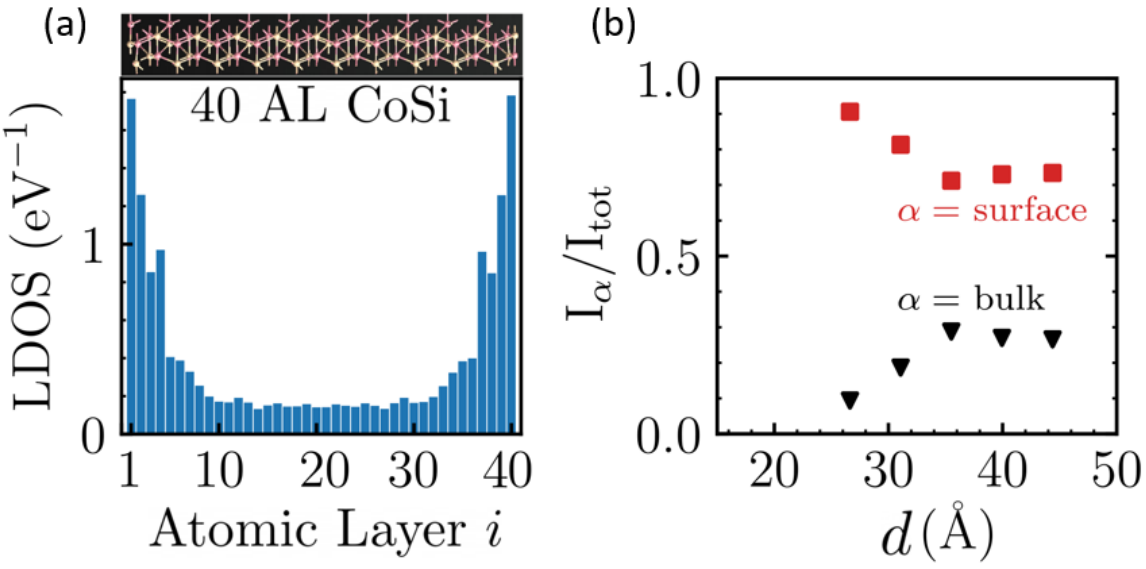

Participation of Fermi-arc surface states in transport of thin CoSi slabs. (a) Local density of states (LDOS) at E_F resolved along the thickness of a 40 atomic-layer (AL) pristine CoSi slab with d = 36.05 Å, showing strong participation of surface states. LDOS is calculated from the expression

$$(LDOS)_{\text{Atomic Layer } i} = \sum_{j\beta} \frac{1}{(2\pi)^2} \int d^2\boldsymbol{k}\, A^i{}_{j\beta}(\boldsymbol{k}, E_F),$$

where i is the atomic layer number, j is index for the atoms in this atomic layer, β is the index for the local atomic orbital on the atoms, and $A^i{}_{j\beta}(\boldsymbol{k}, E_F)$ is the corresponding $\boldsymbol{k}$-resolved spectral weight. **(b)** Thickness dependence of the fraction of charge current (I_α/I_{tot}) carried by the surface and bulk states respectively, indicating the dominance of surface-state mediated transport.

Supplementary Figure 3

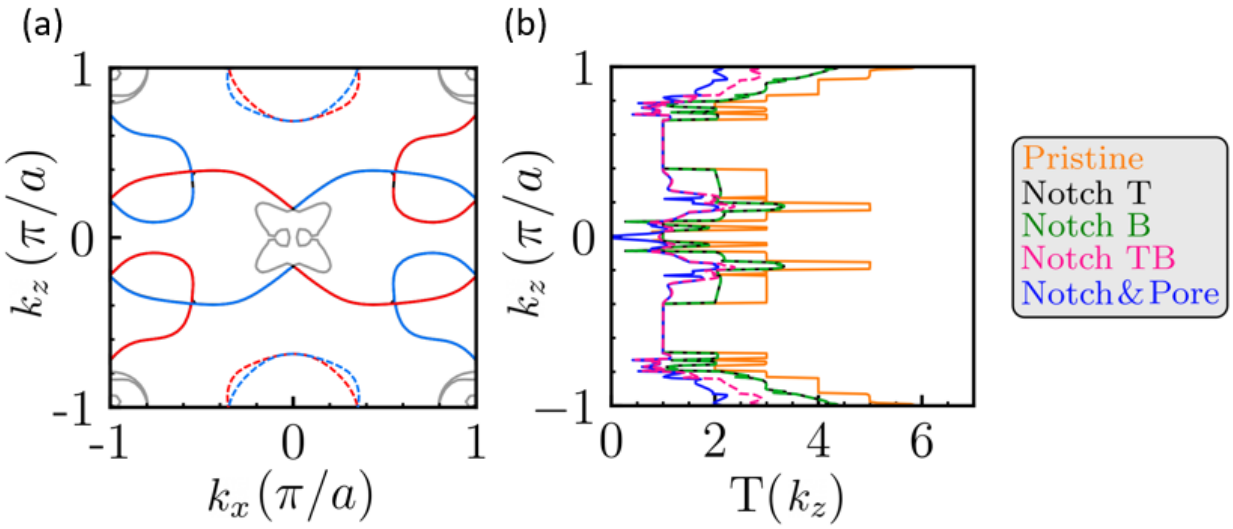

First-principles based quantum transport of CoSi slabs with 1D line defects. (a) Fermi surface of a 40AL CoSi slab with d = 36.05 Å. Surface states originated from the top and bottom surfaces are denoted in red and blue lines, respectively. Gray lines indicate the bulk states. **(b)** The k_z-resolved transmission $T(k_z)$ for 40 AL CoSi slabs with various line defects obtained by NEGF calculations using the QuantumATK package. Orange line denotes the ideal film. Black (Notch T) denotes a slab with a notch on the top surface. Green (Notch B) denotes a slab with a notch on the bottom surface. Pink (Notch TB) denotes a slab with a notch on both the top and the bottom surfaces. Blue (Notch & Pore) denotes a slab with a notch on the top surface and a pore through the bulk.

Supplementary Figure 4

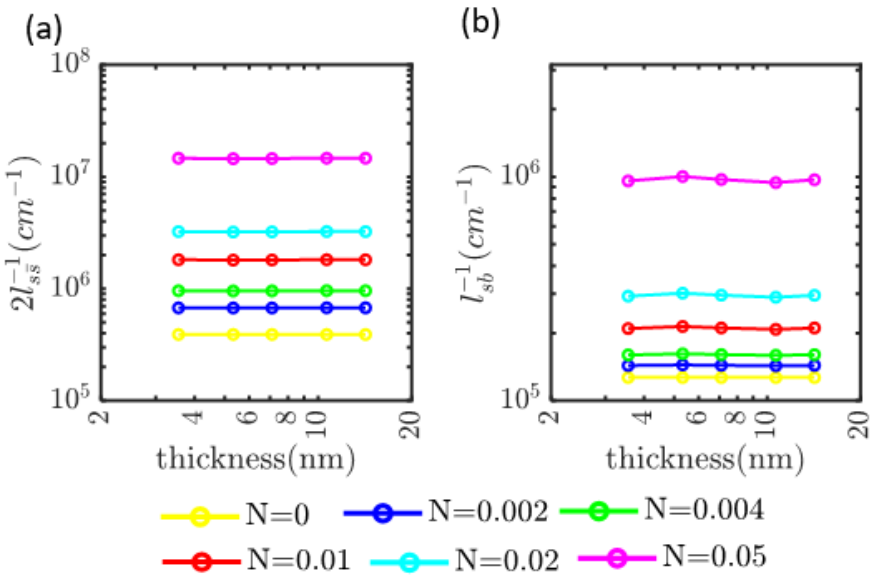

Scaling of scattering lengths with CoSi slab thickness. (a), (b) Calculated surface-to-surface ($l_{s\bar{s}}$) and surface-to-bulk (l_{sb}) scattering lengths for different values of the surface defect density N (see **Methods**). In the range of thickness corresponding to region *I* of Fig. 3, all scattering lengths are thickness independent, and the scattering between time-reversed Fermi arcs on the same surface is stronger than surface-to-bulk scattering. The effective surface scattering length l_s in the main text is obtained by: ${l_s}^{-1} = 2{l_{s\bar{s}}}^{-1} + {l_{sb}}^{-1}$.

Supplementary Figure 5

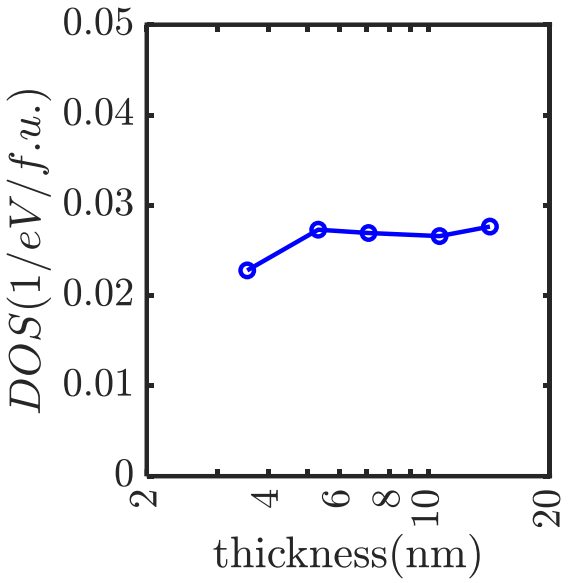

Scaling of density of bulk states with CoSi slab thickness. The calculated density of the bulk states per chemical formula unit (f. u.) at the Fermi level hardly varies in the range of thickness corresponding to region *I* of Fig. 3.

Supplementary Figure 6

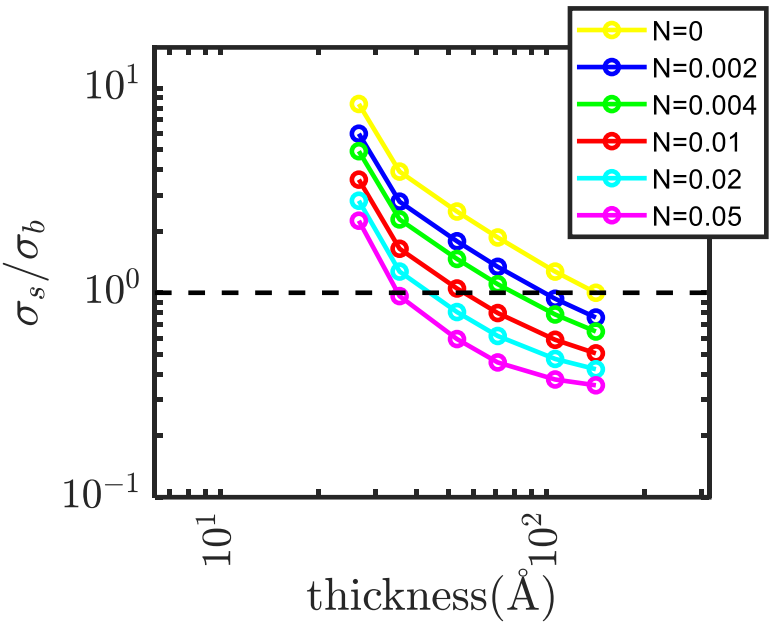

Scaling of surface-to-bulk conductivity ratio with CoSi thickness, calculated from first-principles (see **Methods**) for different values of the surface defect density N in the range of thickness corresponding to region *I* of Fig. 3. With increasing N, σ_s/σ_b decreases, indicative of growing dominance of the bulk states over the surface states, giving rise to the sign change in the slope of ρ/ρ_0 *vs* d in Figure 3.

Supplementary Figure 7

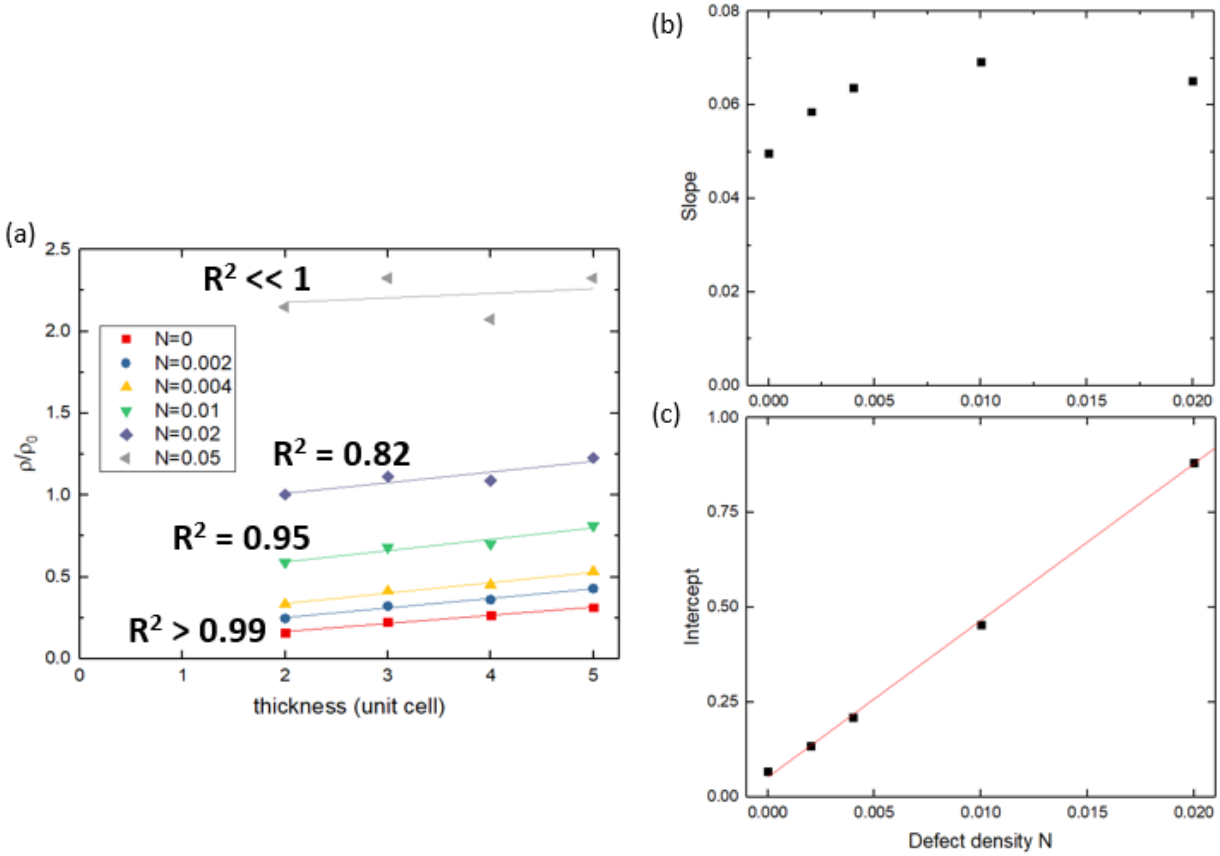

Scaling of normalized resistivity with CoSi thickness in the ultrathin limit. (a) Linear fit to the normalized CoSi slab resistivity calculated from first-principles in the thickness range of region *II* (see Fig. 3 in the main text) for different values of the surface defect density N. For N = 0.02 (equivalent to areal density $\sim 1 \times 10^{13}$ cm^{-2}) and below, linear dependence in thickness fits the data well, with a high coefficient of determination R^2. **(b)** Slope of the linear fit, which varies weakly with N. **(c)** Intercept of the linear fit, which scales linearly with N. These findings are consistent with the approximate equation of $\rho/\rho_0 = \sigma_0/\sigma \propto a\,N + b\,d\,\eta$ proposed for region *II* (see main text).

Supplementary Figure 8

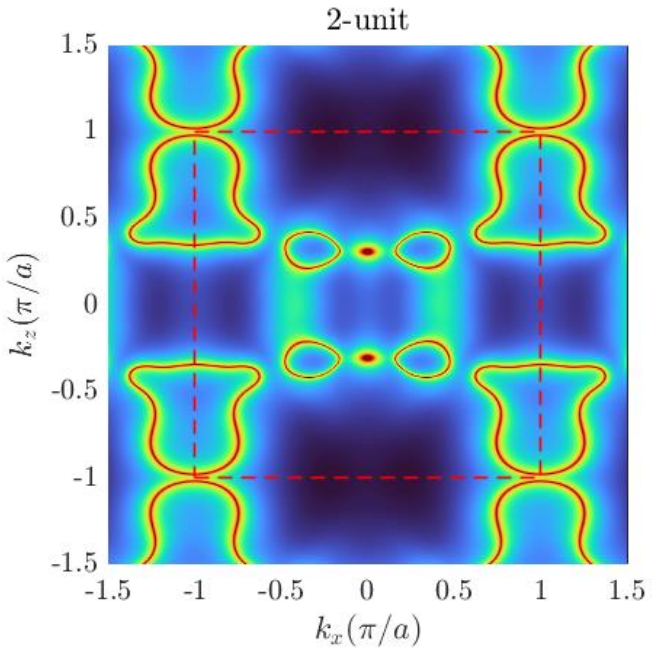

Spectral weight of 2 unit-cell thick CoSi at the Fermi level. First-principles calculations reveal the persistent remnants of the Fermi-arc surface states which preserves the conduction down to the ultrathin limit, resulting in decreasing resistivity with decreasing thickness below the critical thickness.